# The Eucalyptus spectrograph

Antonio Cesar de Oliveira, Beatriz Barbuy, Rodrigo Prates Campos, Bruno Vas Castilho, Clemens Gneiding, et al.

Antonio Cesar de Oliveira, Beatriz Barbuy, Rodrigo Prates Campos, Bruno Vas Castilho, Clemens Gneiding, Antonio Kanaan, David Lee, Jacques R. D. Lepine, Claudia Mendes de Oliveira, Ligia Souza de Oliveira, Francisco Rodrigues, J. M. Silva, C. Strauss, Keith Taylor, "The Eucalyptus spectrograph," Proc. SPIE 4841, Instrument Design and Performance for Optical/Infrared Ground-based Telescopes, (7 March 2003); doi: 10.1117/12.461975

Event: Astronomical Telescopes and Instrumentation, 2002, Waikoloa, Hawai'i, United States

# The Eucalyptus spectrograph

A.C. Oliveira* [a], B. Barbuy** [b], R.P. Campos* [a], B.V. Castilho* [a], C.D. Gneiding* [a], A. Kanaan*** [c], D. Lee**** [d], J. R. D. Lepine ** [b], C. M. Oliveira** [b], L. S. Oliveira* [a], F. Rodrigues* [a], J. M. Silva* [a], C. Strauss** [b], K. Taylor*****
[a]Laboratório Nacional de Astrofísica/MCT, Brazil; [b]Instituto de Astronomia, Geofísica e Ciências Atmosféricas/USP, Brazil; [c]Departamento de Física, UFSC, Brazil; [d]Anglo-Australian Observatory.

## ABSTRACT

As part of the Brazilian contribution to the 4.2 m SOAR telescope project we are building the Integral Field Unit spectrograph, "SIFUS". With the aim of testing the performance of optical fibers with 50 microns core size on IFUs, we constructed a prototype of the IFU and a spectrograph that were installed at the 1.6 m telescope of the Observatório do Pico dos Dias (OPD), managed by Laboratório Nacional de Astrofísica (LNA) in Brazil. The IFU has 512 fibers coupled to a LIMO microlens array (16 x 32) covering a 15"x 30" field on the sky. The spectrograph is a medium resolution instrument, operating in a quasi-Littrow mode. It was based on the design of the SPIRAL spectrograph built by the Anglo-Australian Observatory. The name Eucalyptus was given following the name of the native Australian tree that adapted very well in Brazil and it was given is in recognition to the collaboration with the colleagues of the Anglo-Australian Observatory. The instrument first light occurred in the first semester of 2001. The results confirmed the possibility of using the adopted fibers and construction techniques for the SIFUS. We present the features of the instrument, some examples of the scientific data obtained, and the status of the commissioning, calibration and automation plans. The efficiency of this IFU was determined to be 53% during telescope commissioning tests.

**Keywords:** spectrographs, optical instrumentation, optical fibers, IFU

## 1. INTRODUCTION

The Eucalyptus IFU combines the use of a microlens array with optical fibers. The microlens array provides contiguous spatial sampling, whilst optically coupling the telescope to the fibers at the appropriate focal ratio to maximize throughput. The main components of the Eucalyptus IFU are: the fore-optics, lenslet array, fiber feed and spectrograph. The microlens array is placed at the focal plane of the telescope to sample the two-dimensional image. As is illustrated in Fig. 1, each microlens produces an image of the telescope pupil onto the core of an optical fiber. The two-dimensional array of optical fibers is rearranged to form a one dimensional slit at the entrance to the spectrograph. A spectrum is, therefore, produced for each microlens at the input. The fore-optics was designed for the F/10 cassegrain focus of the 1.6 m LNA telescope. The spectrograph was designed to accommodate 512 fibers. The spectrograph is a quasi-Littrow design and accepts the F/4.8 beam from the fibers.

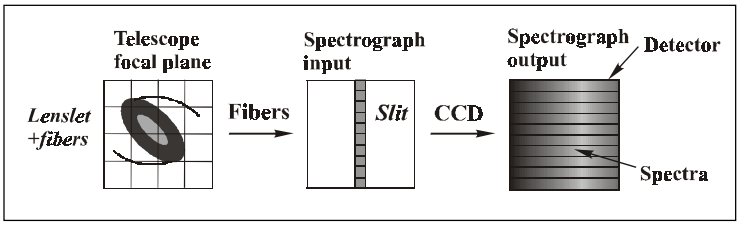


Fig. 1: Scheme of the principle of the operation of the Eucalyptus IFU

* cesar@lna.br; phone 55-35-3623.1500; http://www.lna.br; LNA/MCT, MG/Brazil
** jacques@iagusp.usp.br; 55-11-3091.4762; IAG/USP, SP/Brazil
*** kanaan@fsc.ufsc.br; UFSC, SC/Brazil
**** dl@roe.ac.uk; UKATC, Edinburgh/UK
***** kt@astro.caltech.edu; Caltech, California/USA

The collimated beam size is 150 mm, allowing the diffraction gratings already available at LNA to be used to provide dispersions of 8 – 25 angstrons per millimeter and spectral resolutions up to 4000 in first order. The spectrograph is bench mounted and installed in an controlled environment room. The spectrograph will be used with a 4608 x 2048 pixels Marconi CCD detector (square 13.5 microns pixel). For the commissioning tests we have used a 1024 x 1024 pixel SiTE CCD detector (square 24 microns pixel) so for now, the field is reduced to 9 x 30 arcsec instead 15 x 30 arcsec that is possible to cover by the lenslet. The long axis of the CCD is aligned with the spatial direction, allowing 300 of the 512 optical fibers to be accommodated on the detector. The total length of fiber bundle is 12 m. The use of a fast collimator, which operates at the same focal ratio as the optical fibers, avoids the need for additional microlens array at the output slit. A summary of the characteristics of the Eucalyptus IFU is given in table 1.

| | |
|---|---|
| Number of microlens | 512 |
| Size of microlens | 1 mm |
| Fiber core diameter | 50 microns |
| Spatial sample | 0.93” |
| Field of view | 15” x 30” |
| Total slit length | 37.1 m |
| Magnification of the fore-optics | 13.5 |

Table 1: Characteristics of the Eucalyptus IFU

## 2. DESIGN AND CONSTRUCTION

### 2.1 Microlens array

The lenslet array provides contiguous spatial sampling and images the telescope pupil onto the optical fibers at the appropriate focal ratio. A photograph of the LIMO lenslet array is shown in Fig. 2. The lens focal ratio are F/5.5 (F/3.9 across the diagonal) with a 1.0 mm pitch. The radius of curvature of the cylindrical lens is 2.55 mm with an aspheric term of -0.97. Both cylindrical lenses arrays have the same specification. This kind of microlens array was tested using the techniques described by Lee et al [1]. The point-spread function was found to be consistent with that expected due to diffraction. The lens pitch was measured and confirmed to be 1.0 mm with positioning RMS errors of ~ 2 microns. To reduce chromatic aberration, the silica lens arrays is optically coupled to a SF6 glass substrate to form an achromatic lens, which provides good image quality over wavelength range 450-1000 nm

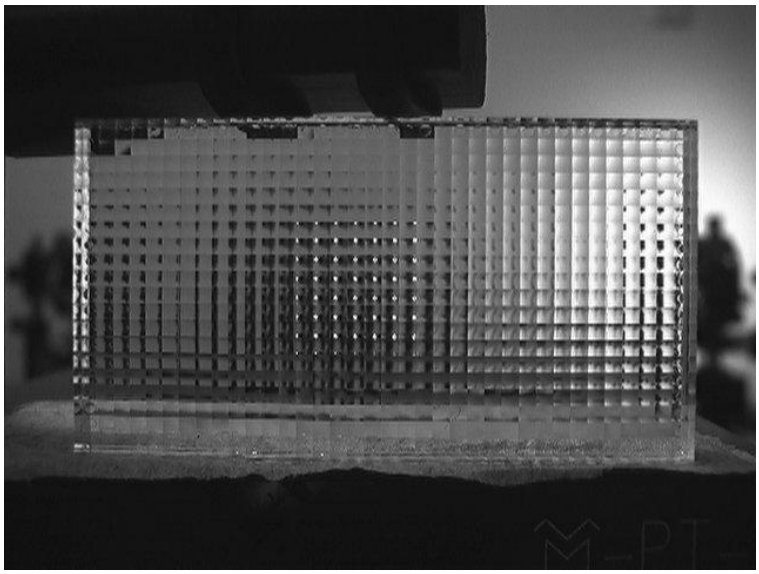

Fig. 2: The array consists of 36 x 20 1mm square lenses although only the central 32 x 16 lenses can be used. Adhesive applied at the outer lenses (small circular droplets in the image) is used to hold the two crossed cylindrical lens arrays together.

### 2.2 Optical fibers

The spatial sampling of an IFU is, $\phi = \alpha D F$, where $\alpha$ is the required sampling interval (in radians) on the sky, D is the diameter of the telescope primary mirror and F is the focal ratio at which the fiber is to operate. For the IFU, a sampling of 0.93 arcsec is required, with D = 1.6 m and F = 5.5, so that a minimum core size of 43 μm is required. When calculating the optimum fiber core size allowance must be made for diffraction, the image quality of the microlens, and errors in the position of the fiber relative to the image formed by the microlens. After taking these factors into account, a core size of 50 μm was chosen for Eucalyptus. By oversizing the fiber core, some error in fiber

positioning can be accommodated, and blurring due to diffraction, without producing significant vignetting of the pupil image. The optical fibers used was made by Polymicro Technologies (model FVPA0500600700200). High $OH^-$ silica fiber was selected to provide the best transmission in the blue (Fig. 3). A dual buffered fiber was chosen: The outer buffer diameters matches the size of the holes in the fiber positioning array (see section 2.3). However, to allow closer packing of the fibers at the output slit, the outer acrylate buffer can be readily removed such that the fibers can be assembled with a spacing determined by the inner polyamide buffer (see section 2.4). In addition, the acrylate buffer makes the fibers more resistant to breakage and, therefore, easier to handle. To ensure that the integral field unit has the maximum throughput it is important to measure the focal ratio degradation (FRD) properties of the optical fiber as this is likely to be the dominant light loss mechanism. The FRD characteristics of the assembled fiber bundles, before attachment of the microlens array, were measured using the technique described by Lee, Haynes & Skeen [2]. A plot of the FRD performance of the Eucalyptus fibers, measured with an F/5.5 input beam at wavelength of 525 ± 50 nm, are shown in Fig. 4. The graphics show that a fraction of the light, between 50 and 70 per cent will be collected by the F/4.8 spectrograph optics. This range was observed with a sample of 25 fibers measured before attach of the microlens. When the fibers are fed with the microlens array, the losses can be expected to be slightly higher due to the faster focal ratios at the corners of the lenses (F/3.9 cf. F/5.5). However, there is some evidence that optically coupling the fibers to glass substrates, as is the case with in this design, reduces FRD [3]. Therefore, the FRD performance of the fiber bundles can be expected to improve when the microlens array and output slit cover glass are attached.

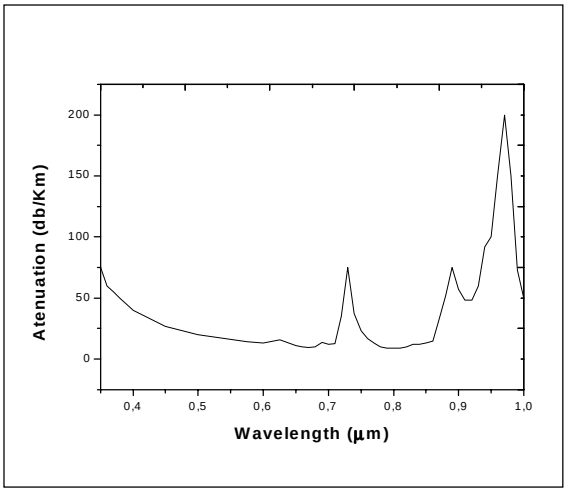


Fig. 3: Spectral attenuation curve for blue fiber between 350 and 1000 nm.

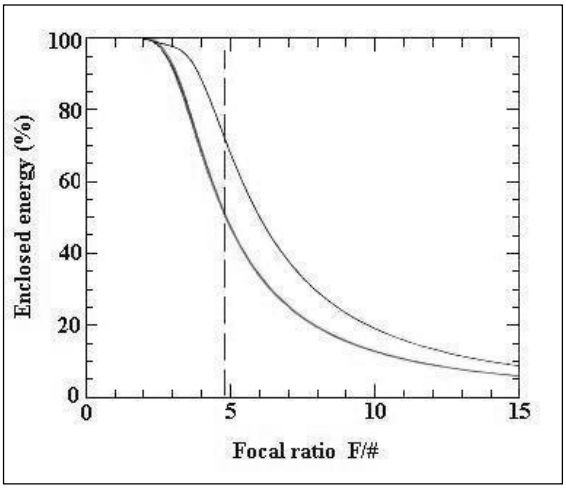


Fig. 4: Plot of the FRD performance of the fibers used in Eucalyptus IFU. The dashed vertical line at F/4.8 is the focal ratio accepted by the spectrograph.

### 2.3 Fiber positioning array

To ensure maximum throughput it is important that the microlens array is accurately aligned with the two-dimensional array of optical fibers. Individual positioning is much time consuming for a large number of fibers and positioning errors are not entirely eliminated. Another approach is to use an array of hexagonally close packed steel tubes [4,5]. An RMS positioning error of 6 μm can be obtained with this technique, but the choice of pitch is limited by the size of tubing available. A different approach was adopted for the IFU with the fibers positioned in array of accurately drilled holes as illustrated schematically in Fig. 5. The fiber positioning array is a grid of 32 x 16 holes spaced on a 1.0 mm pitch. The holes were machine using custom made drills with diameters of 0.60 mm and

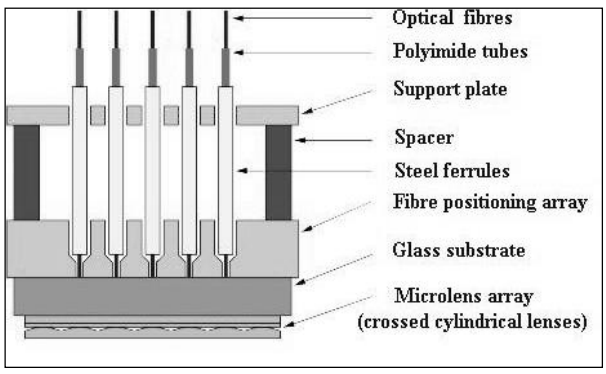


Fig. 5: Layout of the fibers positioning array

0.21 mm. This produces a stepped hole, with the smaller diameter hole used for fiber positioning, while the larger hole is used to accommodate a ferrule. The small holes are approximately 10 μm larger than the fiber diameter to allow sufficient space for an appropriate glue wicking. Using a stepped hole also allows a greater depth of material to be machined than by using a small drill alone. This permits a thicker, hence more robust, piece of material to be used. Both the hole array and support plate were made with tool-makers brass. The machining error in the position of the small holes was measured to be approximately 2 μm RMS.

A support plate is also used, positioned above the fiber positioning array with spacers, in order to maintain accurate angular alignment of the ferrules with respect to the microlens optical axis. Each ferrule contains a polyimide strain relief tube to prevent mechanical stress, and hence FRD, occurring at the point where the fiber enters the ferrule. To secure the fibers, ferrules, and tubes in place, the whole input assembly is immersed in a container of EPOTEK 301-2 adhesive. This epoxy was chosen due to its excellent wicking properties and low shrinkage upon curing. After curing, which takes approximately three days at room temperature, any glue excess is removed prior to optical polishing. Ideally, the optical fibers will be accurately located on a grid of 1.0 mm pitch. However, manufacturing tolerances in the position of the holes, the diameter of the holes, the diameter of the fibers, and the position of the fibers within the holes will all contribute towards an error in the final position. To measure the accuracy of fiber positioning, a lens system was used to re-image the fiber array onto a CCD detector. The position of each fiber in the image was determined using the astronomical image analysis software (IRAF). The final RMS error in fiber position was determined to be 7.5 μm. The distribution of the positioning error is shown in Fig. 6. Note that in extreme cases, positioning errors of up to 20 μm occurred.

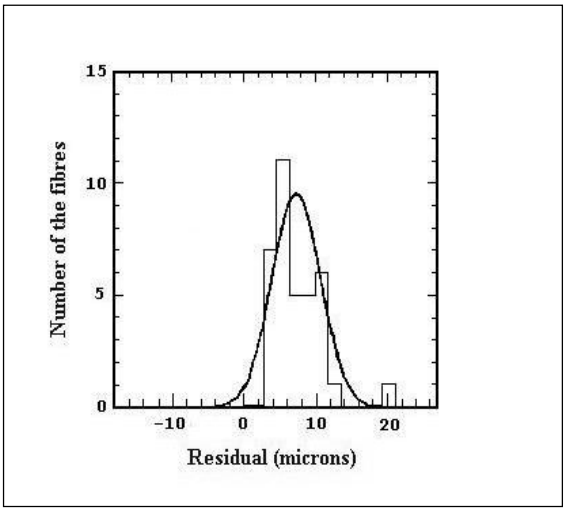


Fig. 6: Histogram plot of the measured error in fibers positions. A sample of 36 fibers was used to get the distribution.

### 2.4 Fiber Output slit

The Eucalyptus IFU fiber output slits consist of 16 brass slitlet blocks each containing 32 optical fibers. The fibers are mounted, buffer side by side, on the slitlet to form a regularly spaced linear array. The 16 slitlet blocks are also mounted side by side to form the output slit. The width of the slitlet blocks is 2.32 mm, corresponding to a total slit length of 37.1 mm. During manufacture, a PTFE clamp is used to hold the 32 fibers in position on the slitlet block whilst the adhesive is applied. Araldite K106 epoxy was used to fix the fibers to the slitlet. After the glue has cured, the PTFE clamp is removed, and the slitlet can be prepared for polishing. By manufacturing the slit in smaller sections, the fibers that have to be manipulated are kept to a manageable number. If breakage's occur it is a simple matter to prepare another slitlet, rather than an entire new slit. Note that although the slits are flat it would be straightforward to arrange the slitlets to approximate a curved slit. During optical tests, the slitlet blocks were identified to be a source of FRD. This may be a result of the close packing of the fibers on the slitlet resulting in mechanical stress. An antireflection coated cover glass is optically coupled to the output slit to reduce the reflection losses at the optical fibers. The index matching optical adhesive reduces the effect of polishing defects on the fiber surface, and hence, reduces FRD losses. The cover glass also prevents the fibers from being scratched.

### 2.5 Protective tubing

The fibers are assembled in the furcation tubing for protection. Each furcation tube contain 32 fibers. The furcation tubing is supplied with a drawstring making it straightforward to draw the fibers through the tube during manufacture. All 16 furcation tubes are placed within a flexible metal conduit for additional protection. The fibers also pass through a spare loop box. This device contains a loop of fiber that can move freely and accommodate any change in length in the conduit without stressing the fibers.

### 2.6 Input field to output slit registration

In order to reconstruct the correct integral field image the registration between the input field and the output slit must be known. The format of the IFU is such that the 16 adjacent rows of 32 fibers at the input are mapped to 16 slitlets at the output. The output slitlets were assembled and then each output slitlet was mapped to the corresponding row in the input field. To achieve this, the complete output slit was mounted on an x-y-z stage and the fibers were sequentially back-illuminated. It is, then, straightforward to identify the illuminated fiber and place it in the correct position at the input.

### 2.7 Optical polishing

To obtain the maximum throughput the surface of the fibers should be polished such that they are optically flat and free from scratches. The polishing process consists of: removal of excess glue with 2000 grit emery paper; initial lapping with 6 μm diamond slurry on a copper plate; second lapping with 1 μm diamond slurry on a tin/lead plate; and final polish with colloidal silica solution on a chemical cloth. The polishing was carried out on a Kent commercial lapping machine, at 60 RPM, using custom made polishing jigs. The optical fibers were inspected with a microscope at all stages of the polishing process to ensure high quality. A photograph of the slit block, after the final polishing, can be seen in Fig. 7 and Fig. 8.

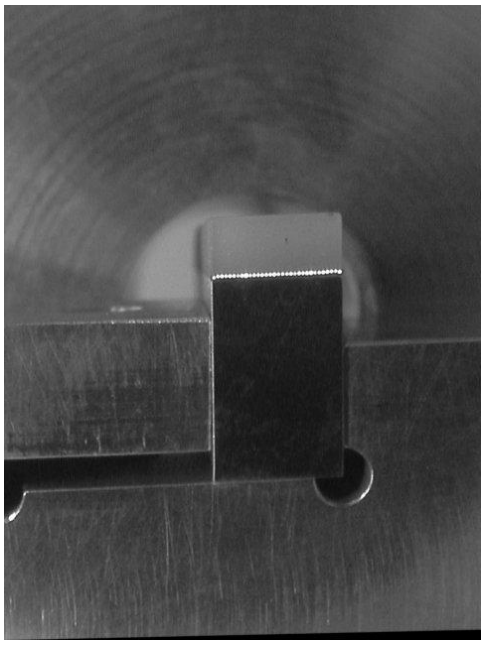

Fig. 7: Photograph of the slit block attached on the jig, after the final polishing.

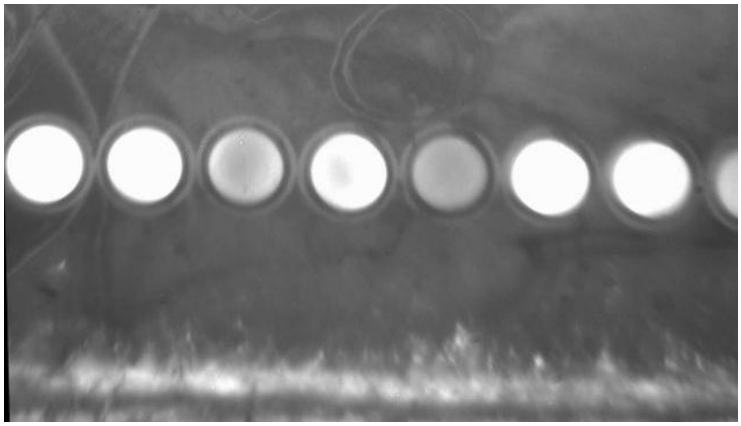

Fig.8: Microscopic image of part of the slit block after the final polishing showing the fibers illuminated.

### 2.8 Fore-optics

The purpose of the fore-optics is to reimage the telescope focal plane onto the microlens array, at the appropriate magnification, so that the microlens subtends $\alpha$ arcsec on the sky. The fore-optics used has a magnification of 13.8 so that the plate scale at the microlens array is 0.93 arcsec/mm. The fore-optics contain three Spindler&Hoyer achromatic lenses. The optical system (Fig. 9) consists of a corrector lens, located at the focal plane of the telescope, a magnification lens, and a field lens located just in front of the microlens array. The field lens ensures that the pupil is located at the infinity such the microlens is illuminated with a telecentric beam. The design provides diffraction limited performance across the

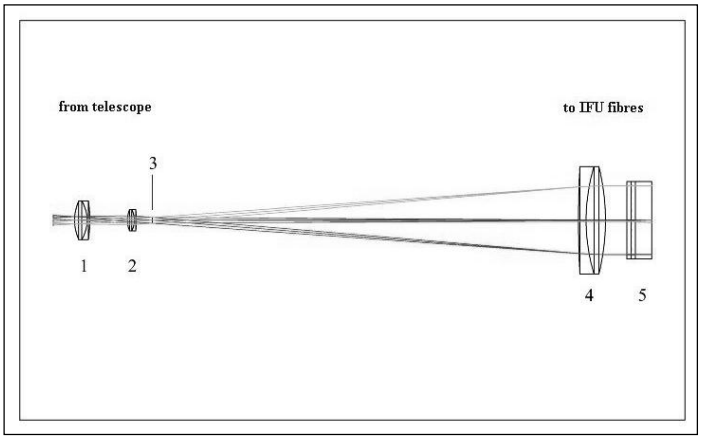


Fig.9: Scheme of the fore-optics system by Zemax software.

entire field of view, for wavelengths 450 – 1000 nm. The lenses are antireflection coated for the range 400 – 700 nm. The telescope is focused on the surface of the first lens. Note that the design of the fore-optics is allows to implement a spectropolarimetric observing mode. This is achieved simply by placing a Wollaston beam splitter at the position of the pupil, just behind the magnification lens. A mask must also be placed at the telescope focal plane. The Wollaston prism, then, forms images in the two polarization states onto the microlens array.

### 2.9 Alignment of the lenslet array with the fiber array

The optical alignment of the microlens array with respect to the two-dimensional array of fibers is critical if high efficiency and uniform throughput is to be obtained. The microlens array is positioned using an x-y rotation mechanism. For alignment purposes, the fiber bundle is back-illuminated and the field lens is used to project an image of the fiber pupil onto a CCD camera. The microlens array is correctly x and y aligned when the pupil image is in the center of the CCD. Alignment errors in x and y are not too critical as the corresponding shift in pupil position can be corrected by an appropriate adjustment of the fore-optics. It is, however, important to achieve accurate rotational alignment of the microlens as an angular misalignment causes a blurring of the projected pupil image. Correct alignment is achieved when the image of pupil is circular. The microlens array was fixed to the fiber bundle using an adhesive which is cured by ultraviolet light (Norland optical adhesive NOA 61). The adhesive remains liquid during alignment and can be cured in a matter of seconds to fix the microlens array in place.

### 2.10 Spectrograph

The Eucalyptus spectrograph has a design similar to the SPIRAL spectrograph, (Fig. 10) [6]. The spectrograph was designed to use the LNA Coudé spectrograph diffraction gratings so a mechanical adaptation was necessary to use the gratings. The Eucalyptus bench spectrograph, (Fig. 11), will be controlled by a standard PC running a C control program under MS-DOS. The telescope Control System will send commands to the PC via a serial port (in the future, will be based on a local Ethernet control network). The diffraction grating rotation is based on a worm gear mechanism (powered by a stepper motor), and rotation angle is accuratly read from an absolute encoder (Heidenhain, ROC 415-5GS6-15B00). The grating angle may be set by the control program or by a custom paddle. The tilt of the CCD, the spectrograph focus will be adjusted by linear actuators (Witec, T-LA28) that are connected to a PC's serial port in a daisy-chain configuration. These actuators have a 28mm travel and an accuracy of +/-8μm with resolution of 0.1μm and repeatability of +/-0.3μm and may be also adjusted manually.

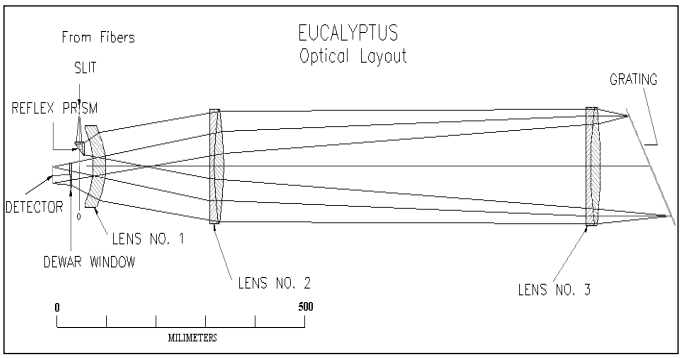


Fig. 10: Optical design of the Eucalyptus spectrograph

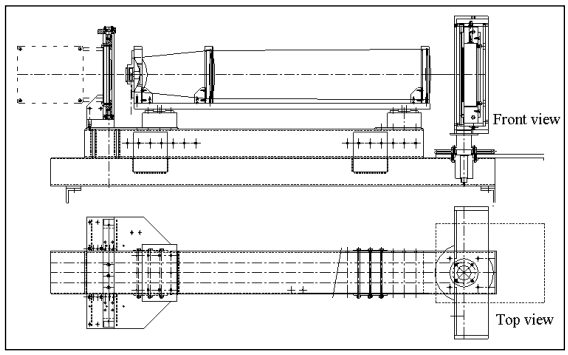


Fig. 11: Mechanical design of the Eucalyptus spectrograph

## 3. COMMISSIONING AND SOFTWARE

### 3.1 Commissioning of the Eucalyptus

Eucalyptus was successfully commissioned on the OPD 1.6 m Telescope during 4 short observational runs, (11/2000), (01/2001), (02/2001) and (04/2001). Initial preparation of the instrument involved mounting and aligning the optics at the telescope focus, installation of the fiber feed, and adjustment of the spectrograph settings. The main problem to attach Eucalyptus IFU on the telescope and critical adjustment was done before the last commissioning run. We constructed a specific mechanics chassis to support the fore-optics system and the IFU input (Fig. 12). The spectrograph

was positioned in the Coudé spectrograph room on the solid pier, (Fig. 13). Observations were done to test and demonstrate the performance of the instrument. We present here an overview of the results from commissioning.

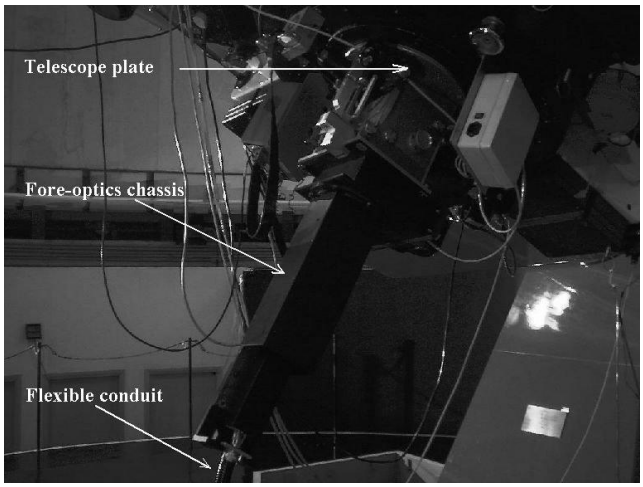


Fig. 12: Eucalyptus IFU attached on the telescope plate.

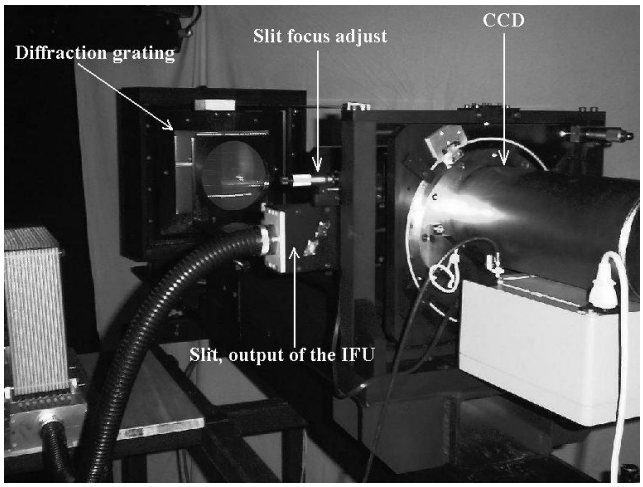


Fig. 13: Eucalyptus IFU attached on the spectrograph.

### 3.2 Data reduction software

The data reduction software for the Eucalyptus (the software will be shared with SIFUS - see Lépine et al. this conference) is under development and will be explained in detail in a forthcoming paper. A beta release should be operational in two months for the first scientific programs with Eucalyptus. Bellow we describe the main features of the software, summarize the main steps of the data reduction procedure and discuss the problem of the superposition of spectra on the CCD. This step of data reduction is described in more detail, as it poses new challenges.

#### 3.2.1 Philosophy and requirements

We intend to provide the means for doing data quick look during the observations and the reduction software to reduce the data during the observing run or at home. The software will be run under IRAF because it is a free and supported platform, and most of Eucalyptus and SIFUS users are familiar with it.

The only step that is specific to Eucalyptus and SOAR-IFU reduction is the extraction of the fiber spectra from the CCD image. It is expected that everything else could be done using standard IRAF packages with minor modifications. As for looking at the final 3D data cube, there are also existing packages that can do this. We developed a task similar to *ldisplay* in the *gmisc* package as a quick look tool.

#### 3.2.2 Reduction Pipeline Steps

Considering that the acquisition system will provide the raw data in FITS.MEF, the steps of the reduction procedure can be summarized as follows:

(a) The images are first processed for bias; flat field and fiber throughput correction; cosmic ray removal; sky subtraction (in the case of nod-and-shuffle).
(b) Extracting the signal from each fiber, by using the multiple-Gaussian fitting code. This step takes a relatively long time to be performed, and a simpler extraction will be provided for a quick view of the results.
(c) Extraction of the spectra in the two dimensional images and their scattered light subtraction and extraction to one-dimensional spectra in multispec format.
(d) Extraction of the comparison lamp spectra and wavelength calibration. In the case of sky subtraction using the sky IFU, it may be preferable to perform sky subtraction after this step, since small wavelength shifts may appear between different regions of the slit.
(e) Writing reduced data on data cube format. The common standard for the data cube file will be a multi-extension FITS file. It is a single 3-D image with the axes in the order x/ra (pixels), y/dec (rows), lambda (planes) and the

basic FITS keywords - CRVAL1, CD1_1, CRPIX1 etc. The logical extension is to have corresponding 3-D variance and data quality images in extra FITS extensions.

From the data cube, it will be straightforward to produce maps of line intensities, for a number of selected lines. For those who are interested in velocity maps (rotation curves of galaxies, kinematics of HII regions, etc), one possibility is to rely on the wavelength calibration already contained in the data cube.

### 3.2.3 Deconvolution of overlapping spectra

In this subsection we discuss step (b) above in more detail, describing the problem of the superposition of spectra on the CCD. To solve this problem we developed a code to fit multiple Gaussians. The code was based on the ROOT routines and tested first with theoretical curves. The procedure tries to fit simultaneously the observed profile of the whole set of fibers. In Fig. 14 the cut of a flat field image obtained with the IFU-prototype is shown. This illustrates how many pixels are contaminated by the signal of the other fibers.

The first step in the calculations is to determine the center and the FWHM of each fiber profile. In principle, the signal of the fiber could be represented by a Gaussian with constant width, which is centered at a fixed position. When these parameters are known, the next step is to fit the real data (representative calibration data). In this case, only the amplitudes of the observed curves are fitted. The final step is to extract the observed signal of each fiber, removing the contamination from the other fibers. A numerical mask should be applied in the case of non-Gaussian profile, in order to correct for the spurious contributions. This could occur in the case of contamination due to the cylindrical curvature of the micro-lens, for example.

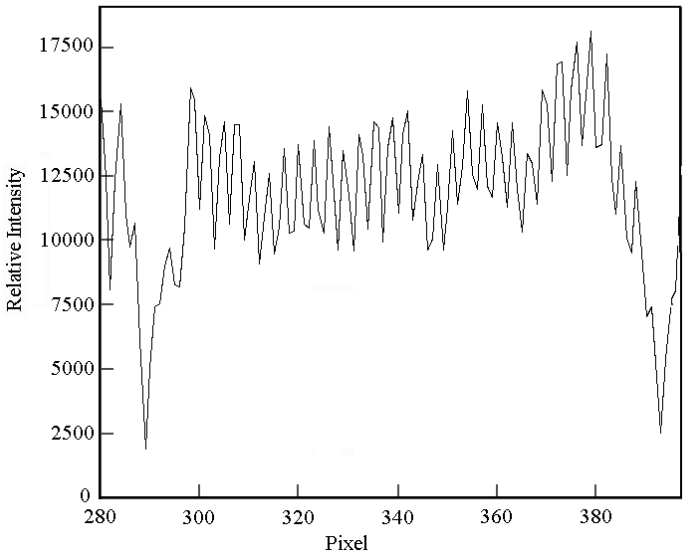


Fig. 14: Cross section of a flat field image perpendicular to dispersion, illustrating the high overlapping of the signal of neighbouring fibers.

If the signal profile of the fibers does not vary appreciably by changing the instrument configuration (changes of gratings, grating angle and camera angle), once the main parameters have been determined, the observed data will be fitted in a fast way. Eventually, a number of files containing the parameters for different configurations could be necessary. Presently we advise the observers to obtain flat field calibrations each evening (for each configuration) before the observations, that will be used for the Gaussians parameter determinations.

Simulations have shown that trying to fit all the Gaussians parameters, even from very good S/N flat field images introduces errors in the solutions. The errors are more important for the cases when the no superposed range is close or smaller than the fwhm of the Gaussian. Those are the cases for both spectrographs (SIFUS 3 pixel, FWHM 3; Eucalyptus: 2k x 4k CCD 5 pixel, FWHM 3.5 pixel and 1k x 1k CCD 3 pixel, FWHM 3 pixel). To solve this problem the center and sigma of the Gaussians should be know in advance.

The simplest case is a single cut across the spatial dimension of the IFU-gram with the light from only a single fiber passing through the spectrograph in order to have the signal intensity and shape (width and center of the Gaussian) measured without contamination from the other fibers. In principle, this procedure should be repeated as many times as the number of pixels in the dispersion direction. However, in practice, the parameters will probably vary linearly in the dispersion direction, and some measurements at different wavelengths will be sufficient to describe the width and center as a function of wavelength. The individual spectra will give us the width and center of the profile of each one of the fibers.

To obtain the calibration data of the individual fibers we designed a mask, which covers one in each five fibers at the microlens array (Fig. 15), providing no contaminated spectra of all fibers in five images. The mask holes are somewhat smaller than the microlenses (0.6mm) to avoid contamination by alignment difficulties.

The last step is to fit the intensity of each fiber profile in the overlapping spectrum (calibration data) and then to apply the previously measured width and centers (Fig. 16). The more complex fit (intensity, width and center) is done first to the calibration data, which has more photons counting and do not suffer from superposition. In this way, the science data have to be fitted for a single parameter (times the number of fibers in one spatial cut). The fit to the science data will give us the intensity of each fiber at every wavelength, by repeating this procedure several times in the dispersion direction.

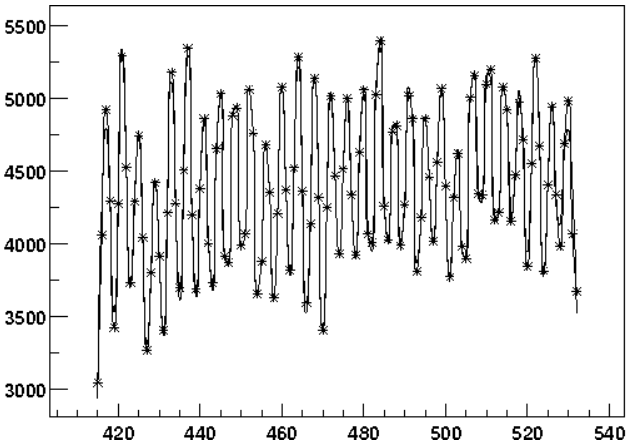


Fig. 16: The fit to the flat field real data – symbols represents the data and the solid line represents the fit

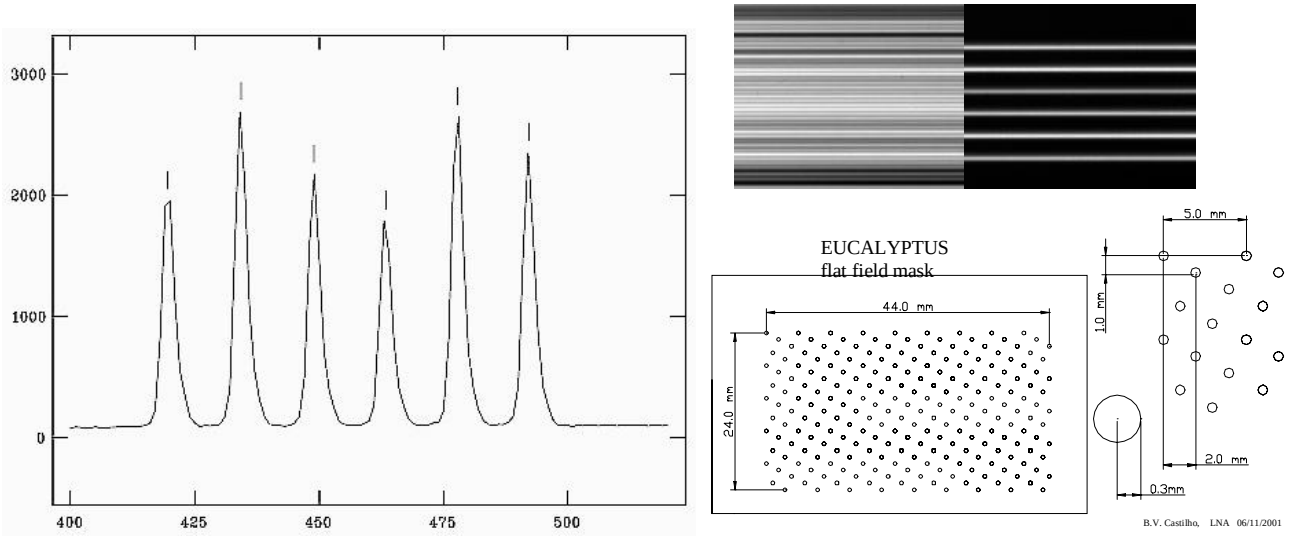


Fig. 15: a) The cross section of a masked flat field image. The mask was used in order to assure that the signal detected by one fiber is not contaminated by the signal of the neighboring fibers. The FWHM is 3.12 pixel. b) Comparison between the unmasked and masked flats, and c) The mask design.

## 4. RESULTS

The Eucalyptus IFU, has been installed at the OPD 1.6m telescope to test the spectrograph using the 600 l/mm grating. Several objects were observed, and flat field and arc comparison data were obtained. The next figures show some of the data, obtained in the observational runs. These results give an idea about the alignment of the fibers, the rough profile of the signal, and the degree of the spectra overlapping in the CCD.

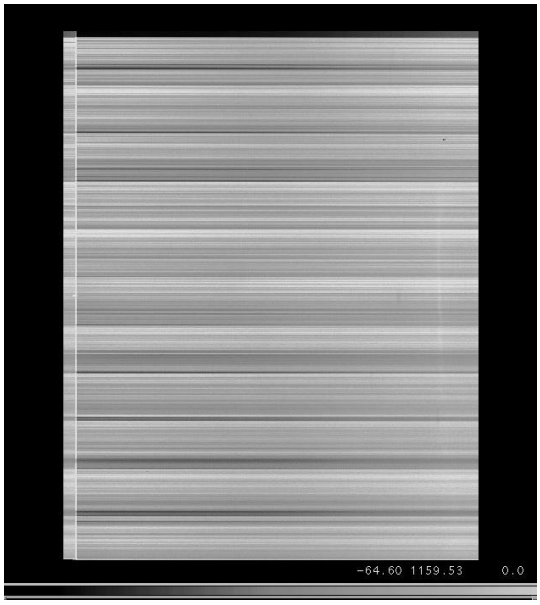


Fig. 17: Flat field white lamp. Image of the fibers of the slit illuminated diffracted by grating on the CCD.

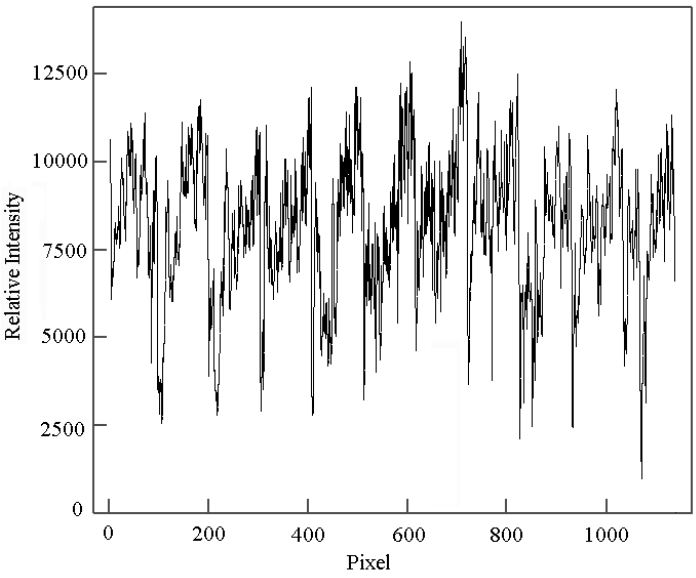


Fig. 18: Spatial cross-section through the IFU flat field spectrum. The line was taken around 610 nm.

Fig. 19: Neon arc lines. Image of the fibers slit illuminated and diffracted by grating on the CCD.

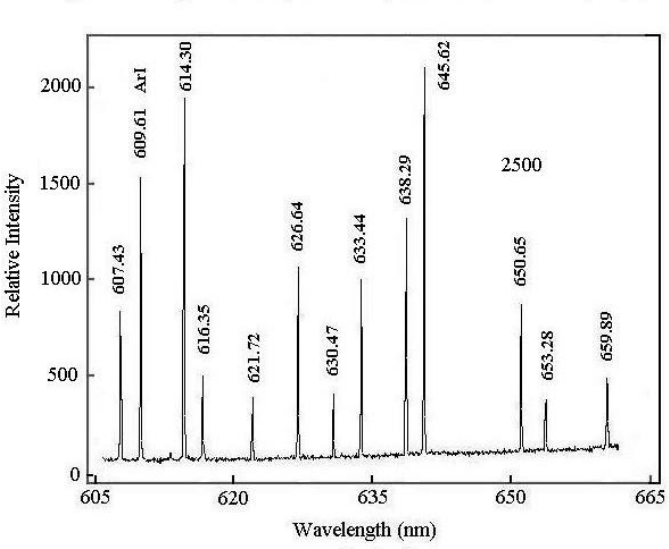


Fig. 20: Spectrum of the Neon arc, between 605 and 665 nm. Cross section of the Neon arc lines of the figure 18.

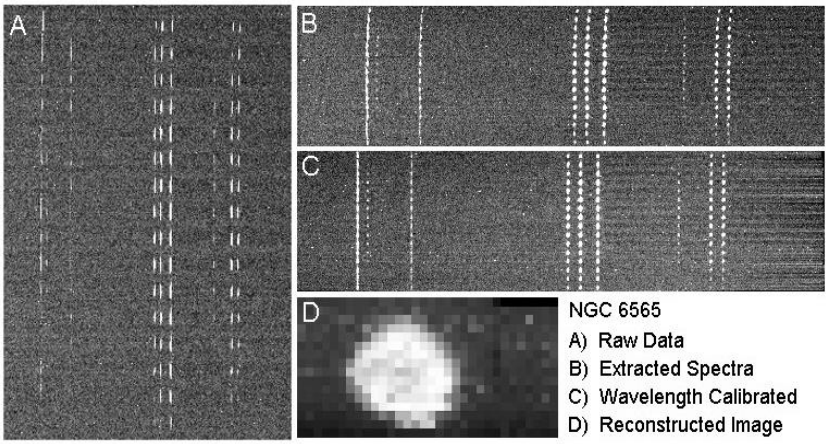


Fig. 21 - Spectra of the planetary nebulae NGC 6565. Four stages of the reduction: a) raw data 512 spectra in the 2k x 4k CCD, dispersion in the x direction; b) extracted spectra; c) the 512 spectra wavelength calibrated (Hα in the center) and d) the reconstructed image from the 512 integrated spectra (32 x 16").

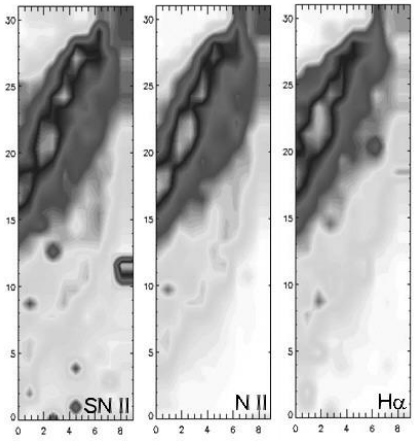


Fig. 22 - Reconstruction of part of the planetary nebulae NGC 3132 in three wavelength regions: a) SN II, b) N II and c) Hα

| | Efficiency |
|---|---|
| Sky | ~ 80 % |
| Telescope | 78 % |
| Fore-optics | 90 % |
| IFU | 53 % |
| Spectrograph | 56 % (without coating) |
| CCD | 60 % (# 106 - at 650nm) |
| Grating | ~ 60 % (at 650nm) |
| Total | 6 % (estimated 11 % with coating + new CCD) |

Table 2: Total spectrograph efficiency.

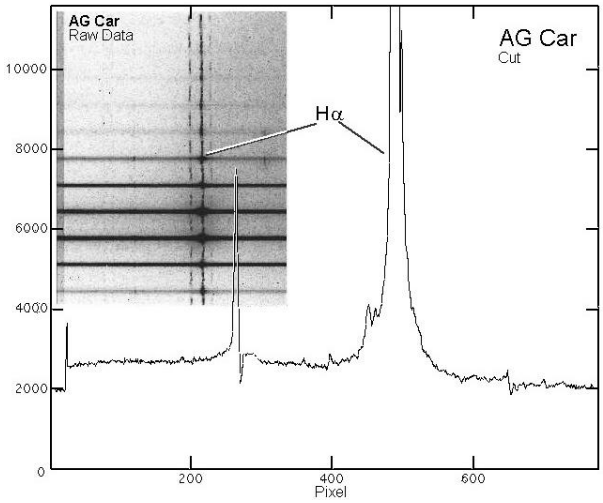


Fig. 23: AG Carinae, 30 s exposure, central wavelength 650nm.

## 5. SUMMARY AND CONCLUSIONS

We described here the design, construction and results obtained for the Eucalyptus IFU. The design uses a crossed cylindrical microlens array coupled on a two dimensional array of 512 optical fibers. The microlens array provides the benefits of contiguous spatial coverage reimaging the telescope pupil at the right focal ratio for use with the fibers. The imaging quality and spectral resolution are as predicted, the components are well aligned, and almost all fibers are correctly positioned with uniform throughput. We are also very pleased that only two of the 512 fibers are broken. The performance of the spectrograph was fully consistent with the ray-tracing expectations. The entire system throughput (including the telescope and atmosphere) was obtained around 6% at 650 nm. The spectrograph provides good focus across the full field, with a compact and symmetrical PSF (~3 pixel FWHM), and the level of scattered light is low. The SIFUS instrument team proposed to use 50 μm core diameter fibers for the SIFUS spectrograph. The construction of the

Eucalyptus, a prototype instrument for SOAR IFU has clearly paid off a means of acquiring the expertise that will be needed to build the SOAR IFU and it is gratifying that a capable scientific instrument has been produced for LNA in the process. The success of Eucalyptus had clearly addressed any doubts about whether an IFU could safely be fabricated using 50 μm core diameter fibers. Data were obtained for a range of astronomical targets, including planetary nebulae, and standard stars. Eucalyptus will be available as a shared risk instrument for the second semester 2002.

## 6. ACKNOWLEDGMENTS

This work was financially supported by the FAPESP project no. 1999/03744-1 and CNPq project 62.0053/01-1-PADCT III/Milenio. We wish like to thank the staff of the Anglo-Australian Observatory, Laboratório Nacional de Astrofísica and Instituto de Astronomia, Geofísica e Ciências Atmosféricas/USP.

## 7. REFERENCES

1. D. Lee, R. Haynes, D. Ren and J. Allington-Smith, "Characterization of Lenslet Arrays for Astronomical Spectroscopy", *PASP* **113**,1406-1419, 2001.
2. D. Lee, R. Haynes and D. J. Skeen, "Properties of optical fibres at cryogenic temperatures", *Mon. Not. R. Astron. Soc*. **326**, 774-780, 2001.
3. J. Schmoll, E. Popow and M. M. Roth, " Focal-ratio Degradation Optimization for PMAS", *in Fiber Optics in Astronomy III*, S. Arribas, E. Mediavilla, and F. Watson, Eds., *ASP Conf. Ser*. **152**, p64, 1998.
4. R. Haynes, D. Lee, J. Allington-Smith, R. Content, G. Dodworth, I. Lewis, R. Sharples, J. Webster, C. Done and R. Peletier, "Multiple-Object and Integral Field Near-Infrared Spectroscopy Using Fibers", *PASP* **111**, 1451-1468, 1999.
5. J. G. Murray, J. R. Allingto-Smith, R. Content, G.N. Dodsworth, C.N. Dunlop, R. Haynes, R.M. Sharples and J. Webster, "TEIFU: a high-resolution integral field unit for the William Herschel Telescope", in Optical and IR Telescope Instrumentation and Detectors, Eds, M. Iye, A.F. Moorwood, **4008**, pp611-622, *SPIE Proceedings Series*, 2000.
6. M.A. Kenworthy, I.R. Parry and K. Taylor, "SPIRAL Phase A: A Prototype Integral Field Spectrograph for the Anglo-Australian Telescope", *PASP* **113**, 215-226, 2001.